

## Noncompeting Channel Approach to Pair Creation in Supercritical Fields

Q. Z. Lv,<sup>1</sup> Y. Liu,<sup>2</sup> Y. J. Li,<sup>1</sup> R. Grobe,<sup>3,4</sup> and Q. Su<sup>2,4</sup>

<sup>1</sup>*State Key Laboratory for GeoMechanics and Deep Underground Engineering,  
China University of Mining and Technology, Beijing 100083, China*

<sup>2</sup>*Beijing National Laboratory for Condensed Matter Physics, Institute of Physics,  
Chinese Academy of Sciences, Beijing 100190, China*

<sup>3</sup>*Max-Planck-Institut für Kernphysik, Saupfercheckweg 1, D-69117 Heidelberg, Germany*

<sup>4</sup>*Intense Laser Physics Theory Unit and Department of Physics, Illinois State University, Normal, Illinois 61790-4560, USA*

(Received 14 June 2013; published 31 October 2013)

The Dirac and Klein-Gordon equations are solved on a space-time grid to study the strong-field induced pair creation process for bosons and fermions from the vacuum. If the external field is sufficiently strong to induce bound states that are embedded in the negative energy continuum, a complex scaling technique of the Hamiltonian can predict the longtime behavior of the dynamics. In the case of multiple bound states this technique predicts the occurrence of a new collective time scale. The longtime behavior of the pair creation is not determined by a single (most important) channel, but collectively by the sum of all individual widths of the embedded states.

DOI: [10.1103/PhysRevLett.111.183204](https://doi.org/10.1103/PhysRevLett.111.183204)

PACS numbers: 34.50.Rk, 03.65.-w, 42.50.-p

It has been predicted [1,2] that intense time-independent external forces can break down the quantum vacuum and create matter-antimatter pairs. Because of the possibility of an experimental verification in the next few years, the area of electron-positron creation in superstrong external fields has become a topic of wide interest [3–9]. In the asymptotically longtime limit [10], the number of created particle pairs can either grow linearly, exponentially, or approach (exponentially) a finite value depending on the force configuration. Many theoretical works [11] have studied the first regime, which occurs for fermions if the corresponding potential that characterizes the field is infinitely extended. Here the growth rate can be obtained directly according to Hund's formula [12] from the corresponding transmission coefficient of the analogous quantum mechanical scattering system. On the other hand, the two exponential regimes are observed if the force field is localized and able to capture the created particles. These supercritical bound states can lead to an exponential growth for bosons while for fermions their occupation is responsible for the termination of the growth. In these regimes Hund's formula cannot be applied to predict the particle yield.

The purpose of this Letter is twofold. First, we will show that the complex coordinate scaling technique [13,14], which is usually used to identify nonrelativistic metastable states [15], can be generalized to predict also quantum field theoretical (QFT) processes that involve the relativistic formation of field-induced bound states. Second, in contrast to known decay or amplification processes of atomic or molecular systems where the longtime behavior is usually predicted by only a single dominant (decay or amplification) channel, the longtime behavior of the quantum field theoretical pair creation is described collectively in a

noncompeting way by the sum of all individual rates. For example, in the case of bosonic exponential growth, the exponent is proportional to the sum of the rates associated with each bound state, and not—as one could expect—associated with the bound state that has the largest individual growth rate. We are not aware of any other physical realization where a similar collective growth rate mechanism characterizes the longtime behavior.

The complex scaling technique itself is a rather well-established computational method for the quantum theory of resonances to calculate the energies and lifetimes of metastable states in atomic, molecular, and chemical systems. It is based on replacing the spatial coordinate  $x$  in the Hamiltonian by a complex one,  $x \exp(i\theta)$ , which rotates the continuous part of the energy eigenspectrum into the complex plane. It turns out that for a suitable chosen phase  $\theta$ , the resulting (non-Hermitian) Hamiltonian can have square integrable eigenstates whose complex eigenvalue describes the energies (real part) and lifetime (inverse of the imaginary part) of the underlying resonances. In this way each resonance can be described separately by an individual state of the scaled Hamiltonian rather than a collection of many continuum states of the original Hamiltonian, necessary for the QFT description of the quantum vacuum. As each resonance is associated with its own characteristic energy and lifetime, we could expect that the longtime limit of any multiresonance fermion system is described by that bound state that has the longest lifetime, corresponding to the smallest imaginary part. However, we will show that if this technique is applied to the pair-creation process, in fact, each imaginary part contributes equally to the longtime limit, independent of its magnitude.

In order to test the predictions of the complex scaling technique, we have solved the Dirac equation (fermions)

and Klein-Gordon equation (bosons) for the quantum field operator on a space-time grid. In the absence of any external force, the continuous energy spectrum is characterized by a mass gap extending from  $-c^2$  to  $c^2$  (in atomic units). If the external binding potential is sufficiently strong, the lowest lying discrete states originating from positive energies can dive into the negative energy continuum [16], as sketched in Fig. 1.

In early pioneering works [17] this “diving” of discrete states into the negative energy continuum was associated with the onset of pair creation, and the energy and the width of the bound states were characterized using Fano-Feshbach type techniques to model the transient excitations induced by the nuclear motion in relativistic heavy ion collisions. However, it is difficult to associate these energy widths directly with any characteristic time scale of the pair creation process. In this Letter, we show that the sum of all of these individual energy widths determines collectively the longtime behavior of pair creation.

To have a concrete working model, we describe the pair-creation dynamics for the fermions and bosons by the one-dimensional Dirac Hamiltonian  $H_D = c\sigma_1 p_x + \sigma_3 c^2 + V(x)$  and Klein-Gordon Hamiltonian [18,19]  $H_{KG} = p_x^2(\sigma_1 + i\sigma_2)/2 + \sigma_3 c^2 + V(x)$ , respectively. Here  $p_x$  is the momentum along the  $x$  axis,  $c$  denotes the speed of light  $c \approx 137$  a.u. and  $\sigma_i$  are the  $2 \times 2$  Pauli matrices. Each state of the Hilbert space is represented by only two spinor components. A reduction from four to only two components is possible for the Dirac system as the potential  $V(x)$  leaves the spin invariant and it is sufficient to focus on only one spin state. The external field of extension  $D$  is modeled by the scalar Sauter-like [1] potential  $V(x) = V_0(\tanh[(x + D/2)/W] - \tanh[(x - D/2)/W])/2$ . The strength  $V_0$  can be increased to control the number of those discrete levels that have dived below the negative energy continuum with energy  $E \leq -c^2$ .

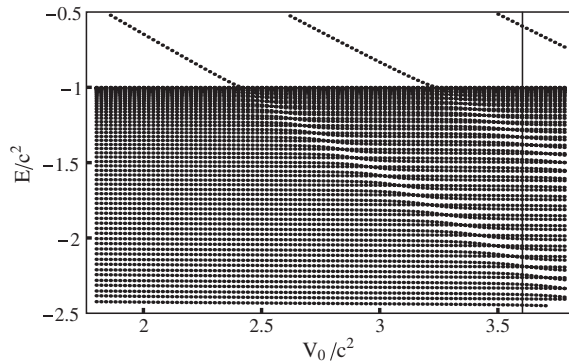


FIG. 1. The energy spectrum as a function of the strength of the external potential. For  $V_0 > 2.42c^2$ , the first discrete state has “dived” into the negative energy continuum. For  $V_0 = 3.6c^2$ , there are two discrete states (close to energies  $E_2 \approx -1.3c^2$  and  $E_1 \approx -2.1c^2$ ) embedded in the negative energy continuum. [ $V(x)$  is given in the text, with  $W = 0.3/c$ ,  $D = 3.2/c$ .]

The energy density associated with  $H_D$  is defined here as  $\rho(E_i) = (|E_i - E_{i-1}|^{-1} + |E_{i+1} - E_i|^{-1})/2$ , where  $E_i$  is the energy level on our numerical space-time grid. The density  $\rho(E)$  displayed in Fig. 2 for parameters [ $W = 0.3/c$ ,  $D = 3.2/c$ ,  $V_0 = 3.6c^2$ ] reveals two bound states that are embedded in the negative energy continuum. Their energies correspond to those locations [ $E_1 = -2.16c^2$  and  $E_2 = -1.33c^2$ ] where the density  $\rho(E)$  is maximum. The corresponding full widths of these peaks at 1, 2, and 3 quarters of the maximum are  $0.007c^2$ ,  $0.005c^2$ ,  $0.003c^2$  for  $E_1$  and  $0.044c^2$ ,  $0.029c^2$ , and  $0.016c^2$  for  $E_2$ , consistently suggesting that the time scales (related to the inverse energy width) associated with each discrete state are rather distinct and differ by a factor of 6. From this assessment one could expect that the longtime dynamics should be dominated by the state associated with energy  $E_1$ . However, quite remarkably, this prediction turns out to be not true.

When we apply the complex scaling technique to our Hamiltonian  $H_D$  we find that among all the continuum states, only the two complex energies  $E_1^* = -2.159c^2 - i0.026c^2$  and  $E_2^* = -1.363c^2 - i0.156c^2$  take negative imaginary parts, whose amounts we denote as  $\kappa_1$  and  $\kappa_2$ . It turns out that the real parts of these two complex energies match within 3% with the centers of the two peaks of  $\rho(E)$  displayed in Fig. 2. Furthermore, the two imaginary parts have a ratio of  $i0.026/i0.156 = 1/6.0$ , in exact agreement with the ratio observed from the analysis of energy density of the real Hamiltonian as in Fig. 2. However, in contrast to the energy density, which can only provide a ratio of the widths, the complex scaling technique gives us also the values for each “width” individually.

In order to examine the dynamical significance of the sum of the two imaginary parts ( $\kappa_1 + \kappa_2 = 0.182c^2$ ) we have to calculate the time evolution of the number of

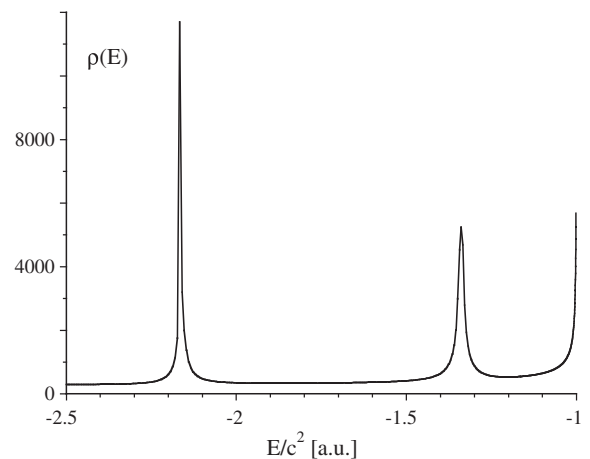


FIG. 2. Energy density  $\rho(E)$  of the total (Hermitian) Hamiltonian  $H_D$  as a function of energy. Two bound states are embedded in the Dirac Sea. The density is peaked at  $E_1 = -2.16c^2$  (with a peak height of 11697) and  $E_2 = -1.33c^2$  (peak height 5246). [ $W = 0.3/c$  and  $D = 3.2/c$  and  $V_0 = 3.6c^2$ .]

created particles  $N(t)$ . Following the usual procedure [20], each single energy eigenstate of the negative energy continuum, defined by  $(H_D - V)|n\rangle = E_n|n\rangle$  (with  $E_n \leq -c^2$ ) was evolved under the full Hamiltonian  $H_D$  [with  $V(x)$ ] leading to  $|n(t)\rangle$ . The time evolution of these states was obtained numerically on a discrete space-time grid using the Fourier transformation based split-operator technique. The average number  $N(t)$  of created particle pairs at time  $t$  can then be calculated by summing over all the transition matrix elements according to  $N(t) = \sum_{p,n} |\langle p|n(t)\rangle|^2$ , reflecting the transitions from the negative energy “Dirac sea” to states with positive energies, defined by  $(H_D - V)|p\rangle = E_p|p\rangle$  (with  $c^2 \leq E_p$ ). The kinetic energy spectrum of the created positrons, is then obtained as  $P(E_k) = \sum_p |\langle p|n(t)\rangle|^2$ , where  $E_k \equiv -c^2 - E_n$  and  $E_n < -c^2$ .

In Figure 3 we show the growth of the particle yield  $N(t)$  for two strengths  $V_0$  of the external potential. There are two distinct temporal regimes that describe  $N(t)$ . For very early time  $N(t)$  grows  $N(t) = \alpha_1 t^2$ . The corresponding proportionality factor  $\alpha_1$  depends on how the potential is turned on in time. For simplicity we have chosen here an instant turn on. The temporal extension of the next time regime [where  $N(t) = \alpha_{II} t$ ] depends on the distance between both wings of the potential  $\approx D$ . A separate space-time resolved analysis showed that particles are dominantly created close to the wings, where the corresponding force [proportional to  $dV(x)/dx$ ] is largest. In this short time region ( $t < D/c$ ) the particles created at each wing do not have sufficient time to travel to the

opposite wing. The corresponding proportionality factor  $\alpha_{II}$  could therefore be obtained from Hund’s rule [12] applied to both wings independently of each other. In the third time region ( $t > D/c$ ) the electrons can visit the opposite particle creation region and begin to reduce the pair creation process due to Pauli blocking. We will focus on this asymptotic longtime regime from now on. For infinite times the pair creation comes to a complete halt [21], reflected by the full occupation of each discrete bound state.

The chosen potential strengths  $V_0$  in the figure lead to one and two bound states. As a result  $N(t)$  approaches 1.2 and 2.24. The deviation from the expected integer value (associated with fully occupied discrete states for one spin) is due to the additional contribution (0.2 and 0.24, respectively) due to the turn on. Independent simulations suggest that this contribution can be minimized by turning the potential on adiabatically.

To obtain a more detailed insight into the functional dependence of  $N(t)$  on  $t$ , we have graphed in the inset of Fig 3 the difference from its asymptotic value  $n(t) \equiv N(t \rightarrow \infty) - N(t)$ . The straight lines on the logarithmic axis show that the longtime limit of the pair creation can be described by a single-exponential behavior,  $N(t) = B[1 - \exp(-\Gamma_B t)]$ , where  $B$  is the number of discrete bound states. For  $V_0 = 2.66c^2$  (single bound state) the exponent is  $\Gamma_1 = 0.08602c^2$ , which agrees with an error of less than 7% with the amount of the imaginary part of the corresponding complex energy for these parameters.

For the more interesting case ( $V_0 = 3.6c^2$  leading to two bound states) the slope is  $\Gamma_2 = 0.17247c^2$ . This longtime exponent agrees, with an error of less than 5%, with the sum of the two imaginary parts,  $\kappa_1 + \kappa_2 = 0.182c^2$ , and not—as one could expect—with only the smaller one  $\kappa_1 (= 0.026c^2)$  associated with the longest lifetime. In our view, this noncompetitive behavior is rather unusual for linear quantum field theoretical systems where typically amplitudes need to be added up (and not multiplied) to obtain physically meaningful quantities.

Both curves are numerically converged but contain similar oscillatory structures, which might be due to the sudden turn-on. They are not so pronounced in  $n(t)$  for  $V_0 = 2.66c^2$  as  $N(t)$  reaches the steady state at later times and therefore the relative difference to the steady state value [denoted by  $n(t)$ ] is larger for graph B than for A.

To obtain some additional insight into the time scales we have displayed in Fig. 4 the corresponding kinetic energy spectrum of the created positrons. While most of the created electrons are trapped in the two bound states, the potential is repulsive for the associated positrons and ejects them to infinity. The corresponding energy spectrum of the positrons is also doubly peaked, with the two maxima at energies  $-c^2 - E_{1,2}$ , where  $E_{1,2}$  match the real parts of the complex energies. While the locations of the peaks have a direct correspondence with the peak positions of

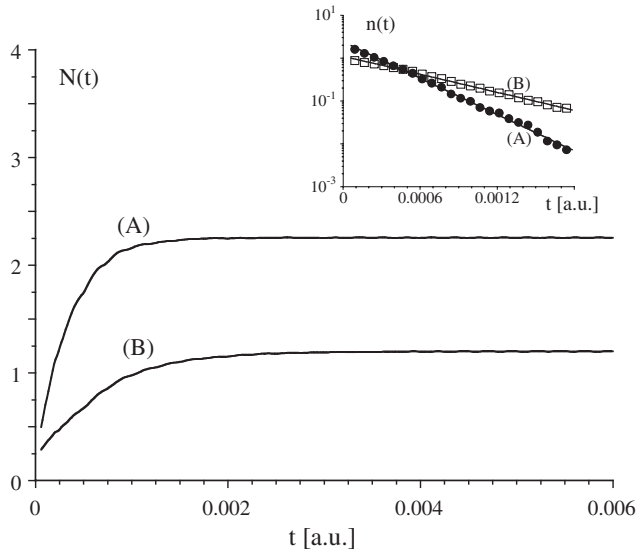


FIG. 3. The final number of created particles as a function of the interaction time for fermions with (A)  $V_0 = 3.6c^2$  and (B)  $V_0 = 2.66c^2$ . The inset presents  $n(t) \equiv N(t \rightarrow \infty) - N(t)$  for longer times with a logarithmic y axis. The slopes of the matched straight lines are  $-0.08602c^2$  and  $-0.17247c^2$ . [The other parameters are  $W = 0.3/c$  and  $D = 3.2/c$ .]

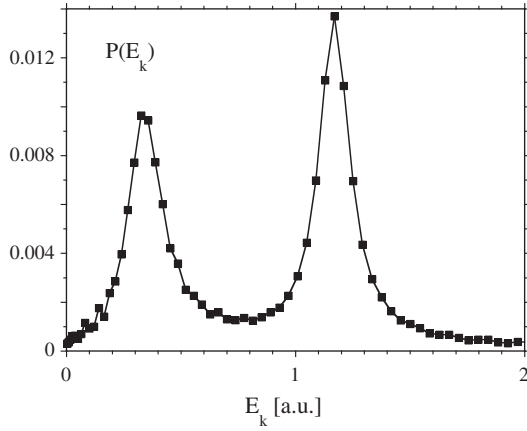


FIG. 4. The positron emission spectrum as a function of the kinetic energy  $E_k$ . [Same parameters as in Fig. 1 and  $T = 5.7 \times 10^{-3}$  a.u.]

the density  $\rho(E)$ , the widths of the peaks, on the other hand, are nearly identical to each other and obviously do not differ by a factor of 6. In fact, the full width at half maximum of both peaks is close to  $0.18c^2$ , suggesting that the positron yield grows at this rate.

In order to test the generality of these findings also for particles with spin zero, we have repeated each of the above simulations for the bosonic pair creation based on the Klein-Gordon Hamiltonian  $H_{\text{KG}}$ . In contrast to the fermionic Pauli-exclusion principle, which shuts off the fermionic pair creation, the occupation of the bound states has exactly the opposite effect on the pair creation for bosons. Bosons that return to the potential regions where they have been created are able to amplify the pair creation process [22]. As a result the creation yield grows exponentially. Once again we would normally expect that only the bound state with the largest imaginary part (amplification rate) should dominate the longtime exponential growth. However, this is again not true.

We have performed the simulation for a potential  $V(x)$  [with  $V_0 = 3.7c^2$ ,  $W = 0.3/c$ ,  $D = 3.2/c$ ] that leads to three bound states in the negative energy continuum. The complex scaling technique applied to these parameters predicts the three complex energies  $E_1^* = -2.378c^2 - i0.076c^2$ ,  $E_2^* = -1.727c^2 - i0.138c^2$ , and  $E_3^* = -1.011c^2 - i0.057c^2$ . The real parts match again the maxima of the corresponding energy density  $\rho(E)$  and predict the locations of the three peaks in the kinetic energy spectrum of the ejected antibosons. More importantly, the numerically observed yield grows here like  $N(t) \sim \exp(0.268c^2 t)$ . This exponent agrees almost perfectly (with a deviation of less than 1%) with the sum of all three imaginary parts ( $0.271c^2$ ), and not just with the largest one, which has the distinctively different value of  $0.138c^2$ .

These findings raise also several interesting questions. For example, the imaginary parts predict both an exponential growth for bosons and an asymptotic approach to

a constant yield for fermions. A general analytical theory that predicts this universal behavior is still lacking. There could be a deeper connection with the “quasibosonic” approximation [23] that leads to a Poisson distribution for the probabilities to produce  $N$  particle pairs. If we tentatively assume that the decay channels are independent of each other, then the probability for the vacuum not to decay is equal to the product of the individual probabilities of not decaying through a particular channel [24]. If these individual survival probabilities are assumed to be exponentials, we would expect that the rate associated with the vacuum survival probability is indeed given by the sum of the individual exponents, as we observe. It is even challenging to model the population growth on a purely phenomenological level by simple nonlinear rate equations, to predict the collective decay or amplification correctly. Also the relationship between the eigenvectors of the complex coordinate scaled system and the bound states for the trapped particles of the original Hermitian Hamiltonian is of interest.

In contrast to common pair creation scenarios (such as potential steps) where the permanent pair creation is usually associated with a degeneracy of energy continua, in our case the pair creation is related to the degeneracy between one (or several) discrete states and the continuum. This situation can occur if the associated external electric field can bind either an electron or positron. For example, the latter can be realized by a superstrong nuclear Coulomb field characteristic of two colliding high- $Z$  ions, where more than just a single bound state can become degenerate with the continuum.

In summary, we have shown that the method based on non-Hermitian Hamiltonians can be generalized to quantum field theory to predict the fermionic as well as the bosonic pair creation yield in a regime, where the external field can induce supercritical bound states. In contrast to a competitive dynamics, the time scale for the longtime behavior is given by the sum of the imaginary parts of those complex energies, whose imaginary part is negative (associated with bound states). As the complex scaling technique requires the diagonalization of the corresponding quantum mechanical (and not field theoretical) Hamiltonian, it can be rather efficiently applied to a wide variety of external field configurations. For example, it could be even applied to study the role of transiently induced discrete states [25].

We enjoyed several helpful discussions with Dr. M. Jiang, Dr. Y.T. Li, Dr. X. Lu, Dr. Z.M. Sheng, Dr. R. Wagner, and Dr. J. Zhang. R.G. would like to thank the group of Professor C.H. Keitel for the nice hospitality at MPIK in Heidelberg. This work was supported by the NSF, by the National Basic Research (973) Program of China (#2013CBA01504), and by the NSFC (Grants No. 10925421, No. 11128409, and No. 11374360).

- [1] F. Sauter, *Z. Phys.* **69**, 742 (1931).
- [2] J. S. Schwinger, *Phys. Rev.* **82**, 664 (1951).
- [3] R. Schützhold, H. Gies, and G. Dunne, *Phys. Rev. Lett.* **101**, 130404 (2008).
- [4] A. R. Bell and J. G. Kirk, *Phys. Rev. Lett.* **101**, 200403 (2008).
- [5] M. Ruf, G. R. Mocken, C. Müller, K. Z. Hatsagortsyan, and C. H. Keitel, *Phys. Rev. Lett.* **102**, 080402 (2009).
- [6] F. Hebenstreit, R. Alkofer, G. V. Dunne, and H. Gies, *Phys. Rev. Lett.* **102**, 150404 (2009).
- [7] S. S. Bulanov, V. D. Mur, N. B. Narozhny, J. Nees, and V. S. Popov, *Phys. Rev. Lett.* **104**, 220404 (2010).
- [8] E. N. Nerush, I. Y. Kostyukov, A. M. Fedotov, N. B. Narozhny, N. V. Elkina, and H. Ruhl, *Phys. Rev. Lett.* **106**, 035001 (2011).
- [9] E. Akkermans and G. V. Dunne, *Phys. Rev. Lett.* **108**, 030401 (2012).
- [10] For early work on bosonic and fermionic pair creation rates, see E. Brezin and C. Itzykson, *Phys. Rev. D* **2**, 1191 (1970); N. B. Narozhny and A. I. Nikishov, *Sov. Phys. JETP* **38**, 427 (1974).
- [11] For a recent review, see, e.g., A. Di Piazza, C. Müller, K. Z. Hatsagortsyan, and C. H. Keitel, *Rev. Mod. Phys.* **84**, 1177 (2012).
- [12] F. Hund, *Z. Phys.* **117**, 1 (1941).
- [13] W. P. Reinhardt, *Annu. Rev. Phys. Chem.* **33**, 223 (1982).
- [14] N. Moiseyev, *Phys. Rep.* **302**, 212 (1998).
- [15] For an application to relativistic systems, see A. D. Alhaidari, *Phys. Rev. A* **75**, 042707 (2007).
- [16] B. Müller, H. Peitz, J. Rafelski, and W. Greiner, *Phys. Rev. Lett.* **28**, 1235 (1972).
- [17] For a review, see, e.g., W. Greiner, B. Müller, and J. Rafelski, *Quantum Electrodynamics of Strong Fields* (Springer Verlag, Berlin, 1985).
- [18] H. Feshbach and F. Villars, *Rev. Mod. Phys.* **30**, 24 (1958).
- [19] For a review on the properties of the Klein-Gordon Hamiltonian, see, e.g., W. Greiner, *Relativistic Quantum Mechanics* (Springer, Berlin, 2000), 3rd ed.; A. Wachter, *Relativistische Quantenmechanik* (Springer, Berlin, 2005).
- [20] For a recent review, see, e.g., T. Cheng, Q. Su, and R. Grobe, *Contemp. Phys.* **51**, 315 (2010).
- [21] P. Krekora, K. Cooley, Q. Su, and R. Grobe, *Phys. Rev. Lett.* **95**, 070403 (2005).
- [22] R. E. Wagner, M. R. Ware, Q. Su, and R. Grobe, *Phys. Rev. A* **81**, 052104 (2010).
- [23] G. Baur, K. Hencken, and D. Trautmann, *Phys. Rep.* **453**, 1 (2007).
- [24] B. R. Holstein, *Am. J. Phys.* **67**, 499 (1999).
- [25] F. Fillion-Gourdeau, E. Lorin, and A. D. Bandrauk, *Phys. Rev. Lett.* **110**, 013002 (2013).